RSC Advances

PAPER

View Article Online
View Journal | View Issue

Check for updates

Cite this: RSC Adv., 2017, 7, 40152

Characterization of blue-excited yellow phosphor $(Y,Ca)_{6+x/3}Si_{11}(N,O)_{21}$:Ce by the bond valence sum model

Takatoshi Seto †[a] and Mikhail G. Brik[bcd]

The new bright yellow phosphor $(Y,Ca)_{6+x/3}Si_{11}(N,O)_{21}$:Ce (CYSON) providing broad emission excited by blue LED is the product of extensive substitution (about 70% of Y) of $Y^{3+} \rightarrow Ca^{2+}$ and $N^{3-} \rightarrow O^{2-}$ in the $Y_6Si_{11}ON_{20}$:Ce parent host, which exhibits a weak emission excited by near UV-excitation only. Such a considerable difference is caused by particular distribution of substituting ions through the crystal lattice sites. For the first time for the title host, these intricate effects have been thoroughly studied in the present paper. We analyzed distribution of cations and their anion surrounding for each of the three Y sites. In addition, the local charge balance was also considered in detail by calculating the Brown's bond valence sum (BVS). The results suggest that the number of oxygen ligands is likely to be 0 at the Y_1 and Y_2 sites, 2–3 at the Ca_1 and Ca_2 sites, 0–1 at the Y_3 site, and 3–4 at the Ca_3 site (the subscript enumerates the inequivalent sites in the CYSON lattice). These data indicate that the Ca ions are likely to be coordinated by a greater number of the oxygen ions than the Y ions, which leads to the conclusion that the Y–N bond should be extensively substituted by the Ca–O bond. Therefore, agglomeration of an increased number of the oxygen ions far away from the Ca^{2+} ions is suppressed. It is suggested that as the bond lengths of the cation–anion pairs in CYSON are much larger than the sum, 2.28 Å, of the ionic radii of the Y^{3+} and O^{2-} ions (which yields a smaller BVS and a small local charge balance), the substituted Ca^{2+}–O^{2-} pair contributes to the stabilization of electric charge distribution. This is the first detailed study of the structural properties of this new phosphor that allowed to identify most probable coordination around each and every cation site in this complicated structure with many inequivalent crystallographic positions.

Received 7th June 2017
Accepted 4th August 2017

DOI: 10.1039/c7ra06382b

rsc.li/rsc-advances

1 Introduction

For about a couple of decades, white phosphor-converted light-emitting diodes (LEDs) have been important devices because they provide an efficient conversion of electric energy to visible light. In addition, they are environmentally friendly, since no toxic Hg is used in their production compared to conventional incandescent and fluorescent lamps.[1] One of the main goals on the phosphor markets is the improved luminous efficacy of novel phosphors for various applications. The phosphors excited by the light of 450 nm-peak of efficient blue LED require a much longer wavelength of excitation than the conventional 254 nm wavelength of the excitation light. The nitridosilicates activated by Eu^{2+} or Ce^{3+} (ref. 2–10) ions are likely to have a strong crystal field splitting (CFS) and a low position of the Eu^{2+} or Ce^{3+} 5d states centroid due to coordination by the N^{3-} ions forming highly covalent chemical bonds. This leads to the enhanced nephelauxetic effect, which in turn decreases the energy difference between the ground 4f and the lowest 5d states of the lanthanide ions. In this case, the longest wavelength of excitation, equivalent to the energy difference between the 4f state and the lowest 5d state, increases.

Seto *et al.* found the new blue-excited yellow phosphor, $(Y,Ca)_{6+x/3}Si_{11}(N,O)_{21}$:Ce,[11] (here and thereafter called CYSON) which has two prominent distinguished features. Firstly, extensive substitution (about 70% of Y) of $Y^{3+} \rightarrow Ca^{2+}$ and $N^{3-} \rightarrow O^{2-}$ in $Y_6Si_{11}ON_{20}$:Ce results in (i) much better crystallinity and (ii) brighter emission under a usual condition of synthesizing nitridosilicate phosphor. The prepared $Y_6Si_{11}ON_{20}$:Ce itself is not a blue-excited phosphor but a near UV-excited phosphor, with much lower crystallinity and weaker emission. The crystal structure of CYSON is shown in Fig. 1. There are three Y^{3+} sites that can be partially substituted by the Ca^{2+} or Ce^{3+} ions and nine sites for the O^{2-}, N^{3-} anions, as shown in Fig. 2.

[a]SETO, 7-3-301, Yukigayaotsuka-machi, Ota-ku, Tokyo, 145-0067, Japan. E-mail: hiroseto@cameo.plala.or.jp
[b]College of Sciences, Chongqing University of Posts and Telecommunications, Chongqing 400065, China
[c]Institute of Physics, University of Tartu, Tartu 50411, Estonia
[d]Institute of Physics, Jan Dlugosz University, Czestochowa PL-42200, Poland
† T. Seto is currently at Advanced Technologies Research Institute, Denka Corporation, while he has done this work at the above address with M. G. Brik.

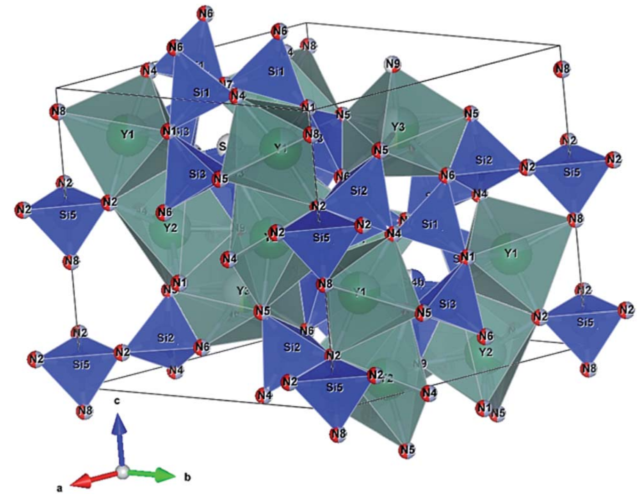

Fig. 1 Crystal structure of $(Y,Ca)_{6+x/3}Si_{11}(N,O)_{21}$:Ce. Y_1, Y_2, and Y_3 indicates three sites of Y or Ca substituted for Y. N_1–N_9 indicates nine sites of nitrogen or oxygen.

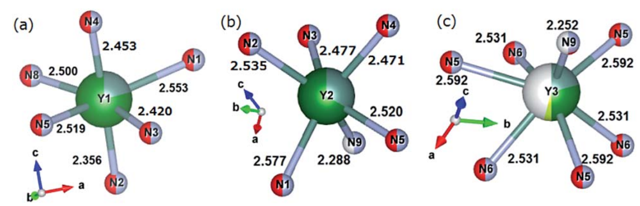

Fig. 2 Coordination of Y_1 site (a), Y_2 site (b), and Y_3 site (c), respectively. Occupancy of Y, Ca, or Ce at each Y_n site is expressed by blue, green, or yellow colours, respectively.

In the present paper we set our goal to investigate whether such extensive and simultaneous substitution provides stable structure from the point of view of the electric charge balance at each cation site. For this purpose, we calculated the Brown's bond valence sum (BVS)[12] for each and every cation site, with and without taking into account effect of the crystal lattice relaxation upon the substitution. The analysis of the obtained results revealed certain peculiar features of coordination of various cations and allowed to understand how such extended cation substitution is realized in the CYSON crystal lattice.

2 Procedure of calculation

The Brown's equation has a wider area of application than the original Pauling's equation on the bond valence sum so far. According to Brown, the bond valence of cation i coordinating anion j can be calculated from the following eqn (1).[12–14]

$$V_i = \sum_j \exp\left[\left(R_{ij} - d_{ij}\right)/B\right] \tag{1}$$

where R_{ij} is the bond valence parameter of a cation i coordinating by an anion j, d_{ij} is the bond length between the cation i and anion j, and B is a constant value (the most reliable value for

Table 1 Occupancies of Y, Ca, and Ce at each site determined by Rietveld refinement[11]

	Ln_1 site	Ln_2 site	Ln_3 site
Y	0.2171	0.3318	0.1978
Ca	0.7764	0.6645	0.3036
Ce	0.0066	0.0038	0.0243

this parameter is 0.37 Å). The bond valence sum can be obtained for each atomic distance, cation species, and species of anion ligands.

We used the values of all d_{ij}, R_{ij}, and B from the reference to the CYSON structure,[11] and Brown's list of the bond balance parameter.[13,14] The R_{ij} value depends on the cation and anion species coordinating a particular cation.

CYSON's space group is $P3_1c$ (no. 159) and its typical composition is $Y_{6+(x/3)-y}Ca_ySi_{11}N_{20+x-y}O_{1-x+y}$:Ce ($x = 1.2, y = 4.5$, Ce molar ratio = 0.06). Each cation's occupancy in CYSON is shown in Table 1,[11] whereas the atomic distances (all in Å) in CYSON are shown in Table 2.[11] It is seen that the Y^{3+}, Ca^{2+}, or Ce^{3+} ions can occupy all three cationic sites. Taken together with anion substitution, this makes an analysis of the structural properties of this phosphor to be a non-trivial problem.

The bond valence parameters R_{ij} used in the present calculation are 2.17 (R_{ij} for the Y–N pair), 2.14 (Ca–N), 2.019 (Y–O), and 1.967 (Ca–O).[13,14] Strictly speaking, due to the partial occupancies of the crystal lattice sites in CYSON it is not known how many N^{3-} or O^{2-} anions coordinate each of the Y^{3+}, Ca^{2+}, or Ce^{3+} ions, respectively. To eliminate any ambiguity in this important issue and understand better the reasons for the improved crystallinity and enhanced luminescence of the substituted phosphor, we considered all possible cases of the N^{3-} or O^{2-} configurations coordinating every Y^{3+} or Ca^{2+} cation at each Ln_q site. As Ln_1, Ln_2, and Ln_3 sites receive 6, 6, and 7 anion ligands, respectively (Fig. 2), there are 2^6, 2^6, and 2^7

Table 2 Atomic distances determined by Rietveld refinement[11]

Ln_1 site:	Ln_1–$(O/N)_1$	2.553(3)	Si_1 site: Si_1–$(O/N)_1$	1.693(5)
	Ln_1–$(O/N)_2$	2.356(4)	Si_1–$(O/N)_4$	1.695(3)
	Ln_1–$(O/N)_3$	2.420(3)	Si_1–$(O/N)_6$	1.798(5)
	Ln_1–$(O/N)_4$	2.453(4)	Si_1–$(O/N)_7$	1.781(2)
	Ln_1–$(O/N)_5$	2.519(1)	Si_2 site: Si_2–$(O/N)_2$	1.665(3)
	Ln_1–$(O/N)_8$	2.500(3)	Si_2–$(O/N)_4$	1.757(5)
Ln_2 site:	Ln_2–$(O/N)_1$	2.577(3)	Si_2–$(O/N)_5$	1.678(5)
	Ln_2–$(O/N)_2$	2.535(3)	Si_2–$(O/N)_6$	1.816(4)
	Ln_2–$(O/N)_3$	2.477(4)	Si_3 site: Si_3–$(O/N)_1$	1.754(5)
	Ln_2–$(O/N)_4$	2.471(2)	Si_3–$(O/N)_3$	1.722(3)
	Ln_2–$(O/N)_5$	2.520(4)	Si_3–$(O/N)_5$	1.823(3)
	Ln_2–$(O/N)_9$	2.288(2)	Si_3–$(O/N)_6$	1.690(5)
Ln_3 site:	Ln_3–$(O/N)_5$	2.592(1)	Si_{4a} site: Si_{4a}–$(O/N)_3 \times 3$	1.684(6)
	Ln_3–$(O/N)_5$	2.592(1)	Si_{4b}–$(O/N)_9$	1.916(2)
	Ln_3–$(O/N)_5$	2.592(1)	Si_{4b} site: Si_{4b}–$(O/N)_3 \times 3$	1.665(3)
	Ln_3–$(O/N)_6$	2.531(4)	Si_{4b}–$(O/N)_7$	2.218(11)
	Ln_3–$(O/N)_6$	2.531(4)	Si_5 site: Si_5–$(O/N)_2 \times 3$	1.797(3)
	Ln_3–$(O/N)_6$	2.531(4)	Si_5–$(O/N)_8$	1.648(8)
	Ln_3–$(O/N)_9$	2.252(7)		

Table 3 Parts of all 64 cases that nitrogen or oxygen coordinates each Y or Ca of Ln_1 site

	Species of anion ligand (the above: case number)												
Cation–(anion)$_{\text{site no.}}$	1	2	3	4	5	6	7	8	9	…	61	62	63	64
Y–(O/N)$_1$	N	O	N	N	N	N	N	O	O	…	O	O	N	O
Y–(O/N)$_2$	N	N	O	N	N	N	N	O	N	…	O	N	O	O
Y–(O/N)$_3$	N	N	N	O	N	N	N	N	O	…	N	O	O	O
Y–(O/N)$_4$	N	N	N	N	O	N	N	N	N	…	O	O	O	O
Y–(O/N)$_5$	N	N	N	N	N	O	N	N	N	…	O	O	O	O
Y–(O/N)$_8$	N	N	N	N	N	N	O	N	N	…	O	O	O	O
Ca–(O/N)$_1$	N	O	N	N	N	N	N	O	O	…	O	O	N	O
Ca–(O/N)$_2$	N	N	O	N	N	N	N	O	N	…	O	N	O	O
Ca–(O/N)$_3$	N	N	N	O	N	N	N	N	O	…	N	O	O	O
Ca–(O/N)$_4$	N	N	N	N	O	N	N	N	N	…	O	O	O	O
Ca–(O/N)$_5$	N	N	N	N	N	O	N	N	N	…	O	O	O	O
Ca–(O/N)$_8$	N	N	N	N	N	N	O	N	N	…	O	O	O	O
Number of oxygen in 6 ligands	0	1	1	1	1	1	1	1	1	…	5	5	5	6

Table 4 Example of the BVS and the difference between BVS and cation's valence (charge imbalance) calculated in case no. 9 (one of all 64 cases of N/O coordination)

	R	d_{ij} (Å)	BV		R	d_{ij} (Å)	BV
Y_1–O_1	2.019	2.553	0.236	Ca_1–O_1	1.967	2.553	0.223
Y_1–N_2	2.17	2.356	0.604	Ca_1–N_2	2.14	2.356	0.514
Y_1–O_3	2.019	2.42	0.338	Ca_1–O_3	1.967	2.42	0.319
Y_1–N_4	2.17	2.453	0.465	Ca_1–N_4	2.14	2.453	0.396
Y_1–N_5	2.17	2.519	0.389	Ca_1–N_5	2.14	2.519	0.331
Y_1–N_8	2.17	2.5	0.410	Ca_1–N_8	2.14	2.5	0.349
BVS			2.442				2.131
Charge imbalance			0.558 (=3 − 2.442)				0.131 (=2.131 − 2)

possible configurations of nitrogen and/or oxygen ligands coordinating the Ln_1, Ln_2, and Ln_3 sites, respectively.

As an example, Table 3 shows just a few anion arrangements out of all 64 cases of the nitrogen or oxygen coordination around the Y^{3+} or Ca^{2+} cations at the Ln_1 site. Table 4 shows the typical results of the BVS calculations for the case no. 9 from Table 3 (one of all 64 cases), including the difference between the BVS and cation's valence, which is called the value of charge imbalance here. All other cases can be calculated in a similar way and are not shown here for the sake of brevity. We present all the calculated results in the next section in the form of diagrams.

3 Results and discussion

Fig. 3(a)–(c) show all the values of the calculated charge imbalance at the Ln_1, Ln_2, and Ln_3 sites, respectively. The smallest value of charge imbalance is obtained in the case of all nitrogen ligands, if the Y^{3+} ions occupy the Ln_1, Ln_2, and Ln_3 sites, whereas when the Ca^{2+} ions occupy the same sites, the smallest value is obtained in the case of 3 oxygen and 3 nitrogen ligands for the Ln_1 and Ln_2 sites, and in the case of 4 oxygen and 3 nitrogen ligands for the Ln_3 site. To understand the conditions that minimize the charge imbalance all the sets of the O^{2-} and N^{3-} ligands providing the smallest three values of charge imbalance are shown in Table 5. The minimal values of charge imbalance are relatively high, 0.2688, 0.3016, and 0.1120 for the Y_1, Y_2, and Y_3 sites, while the same values are much smaller, 0.0037, 0.0049, and 0.0014 for the Ca_1, Ca_2, and Ca_3 sites.

We may take another consideration that the atomic distance determined by the Rietveld analysis in Table 2 (ref. 11) may be an average of the corresponding distances for the Y^{3+}-anion, Ca^{2+}-anion, and Ce^{3+}-anion. Then the actual distances for these three cation–anion sets may be slightly deviating from the average distance. For simply clarifying the behaviour of the substitution, $Y^{3+} \rightarrow Ca^{2+}$ and $N^{3-} \rightarrow O^{2-}$, the Ce^{3+}-anion pair is neglected due to a tiny contribution of the Ce ions (because of low concentration) to the average distance. To account for a difference between the interionic distances, we use the following approach. For the quantitative estimation of the 5d-level energies of the Ce^{3+}-activated phosphors Dorenbos[15] assumed that the phosphor's anions relax radially inward or outward by half the difference ΔR between the ionic radius of the cation A and the ionic radius of the cation B for which the cation A substitutes. As the next step, we take the Dorenbos

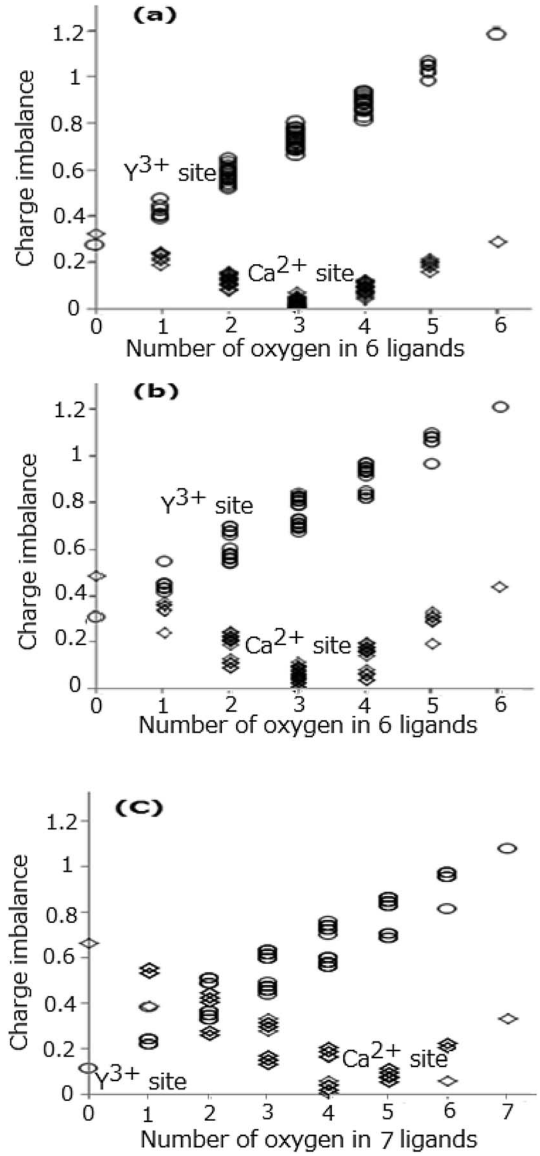

Fig. 3 Difference (charge imbalance) between BVS and cation's valence at Ln_1 site (a), Ln_2 site (b), and Ln_3 site (c), respectively.

assumption, where the difference in distance between the Y^{3+}-anion and Ca^{2+}-anion pairs in the CYSON crystal should be $0.5\Delta R = 0.5 \times 0.10$ Å because the corresponding Shannon radii are 0.90 Å (Y^{3+}, coordination number (CN):6), 1.00 Å (Ca^{2+}, CN:6), 0.96 Å (Y^{3+}, CN:7), and 1.06 Å (Ca^{2+}, CN:7). We take the distance in the Y^{3+}-anion pair as (-0.025 Å + the distance of Ln_x-anion in Table 2) and the distance in the Ca^{2+}-anion pair as (0.025 Å + the distance of Ln_x-anion in Table 2), where the 0.05 Å value (half of the difference in distance between Y^{3+}-anion and Ca^{2+}-anion) can be obtained from a relation [0.025 Å $-$ (-0.025 Å)]. The BVS and the value of charge imbalance are calculated from these values of reasonably re-estimated in such way cation–anion distances. Fig. 4(a)–(c) show all the values of charge imbalance at the Ln_1, Ln_2, and Ln_3 sites originated from the modified bond distance, respectively. The sets of the O^{2-} and N^{3-} ligands providing the smallest three values of charge imbalance are shown in Table 6. The smallest value of charge imbalance significantly decreases from 0.2688 to 0.0779 (Y_1 site), from 0.3016 to 0.1131 (Y_2 site), and from 0.1120 to 0.0247 (Y_3 site) when the two Y^{3+}-anion and Ca^{2+}-anion distances at the same site are modified taking into account differences of the ionic radii in the corresponding pairs. The coordination number of oxygen yielding the smallest value of charge imbalance is slightly changed from 3 to 2 (Ca_1 and Ca_2 sites), from 4 to 3 (Ca_3 site), from 0 to 1 (Y_3 site).

Table 5 The sets of O^{2-} and N^{3-} ligands providing the smallest values of charge imbalance

Sets of Y^{3+}/Ca^{2+}–O^{2-}/N^{3-}	Values of charge imbalance
Y_1–[N_1, N_2, N_3, N_4, N_5, N_8]	0.2688
Y_1–[O_1, N_2, N_3, N_4, N_5, N_8]	0.3877
Y_1–[N_1, N_2, N_3, N_4, O_5, N_8]	0.3992
Ca_1–[O_1, O_2, N_3, O_4, N_5, N_8]	0.0037
Ca_1–[N_1, O_2, N_3, O_4, O_5, N_8]	0.0040
Ca_1–[O_1, O_2, O_3, N_4, N_5, N_8]	0.0060
Y_2–[N_1, N_2, N_3, N_4, N_5, N_9]	0.3016
Y_2–[O_1, N_2, N_3, N_4, N_5, N_9]	0.4131
Y_2–[N_1, O_2, N_3, N_4, N_5, N_9]	0.4265
Ca_2–[O_1, O_2, N_3, N_4, N_5, O_9]	0.0049
Ca_2–[O_1, N_2, N_3, N_4, O_5, O_9]	0.0101
Ca_2–[N_1, O_2, N_3, N_4, O_5, O_9]	0.0239
Y_3–[N_5, N_5, N_5, N_6, N_6, N_6, N_9]	0.1120
Y_3–[N_5, N_5, O_5, N_6, N_6, N_6, N_9]	0.2191
Y_3–[N_5, O_5, N_5, N_6, N_6, N_6, N_9]	0.2191
Ca_3–[N_5, N_5, N_5, O_6, O_6, O_6, O_9]	0.0014
Ca_3–[N_5, N_5, O_5, N_6, O_6, O_6, O_9]	0.0182
Ca_3–[N_5, O_5, N_5, N_6, O_6, O_6, O_9]	0.0182

On total consideration including both cases of the same distance (Table 2) and the different distances, the number of the oxygen ligands seems to be 0–1 at the Y sites and 2–4 at the Ca sites, which suggests that the Ca ions are likely to be coordinated by more oxygen ions than the Y ions. The result coincides with the rough but essential Pauling's second rule[16] where O^{2-} should be substituted for the N^{3-} site near the Ca^{2+} ions rather than near Y^{3+} ions because it can minimize the local volume where the sum of electric charge, -1, caused by the $Y^{3+} \rightarrow Ca^{2+}$ substitution, is localized. The ratio O/(O + N) is likely to be 0% at Y^{3+}, 33–50% at Ca^{2+} at the Ln_1 and Ln_2 sites, 0–14% at Y^{3+}, 43–57% at Ca^{2+} at the Ln_3 site. Then, on the consideration of occupancies of (Y + tiny amount of Ce) and Ca in Table 1, the average ratio O/(O + N) is likely to be 26–39% at Ln_1 site, 22–33% at Ln_2 site, and 25–39% at Ln_3 site, respectively. Total ratio of O/(O + N) in CYSON is (1–1.2 + 4.5)/21 = 21%, which is roughly at the same level with the above ratios in all three Ln sites.

Table 2 and Fig. 1 shows that there are six four-fold coordinated sites for the Si^{4+} ions (Si_1, Si_2, Si_3, Si_{4a}, Si_{4b}, Si_5). We also calculated the BVS and the values of charge imbalance for these Si sites, which are shown in Table 7. The minimum value of charge imbalance is obtained for the Si–(O, N, N, N) composition in almost every Si site in CYSON. It means that the ratio O/(O + N) at Si sites, ~25%, providing the minimum instability

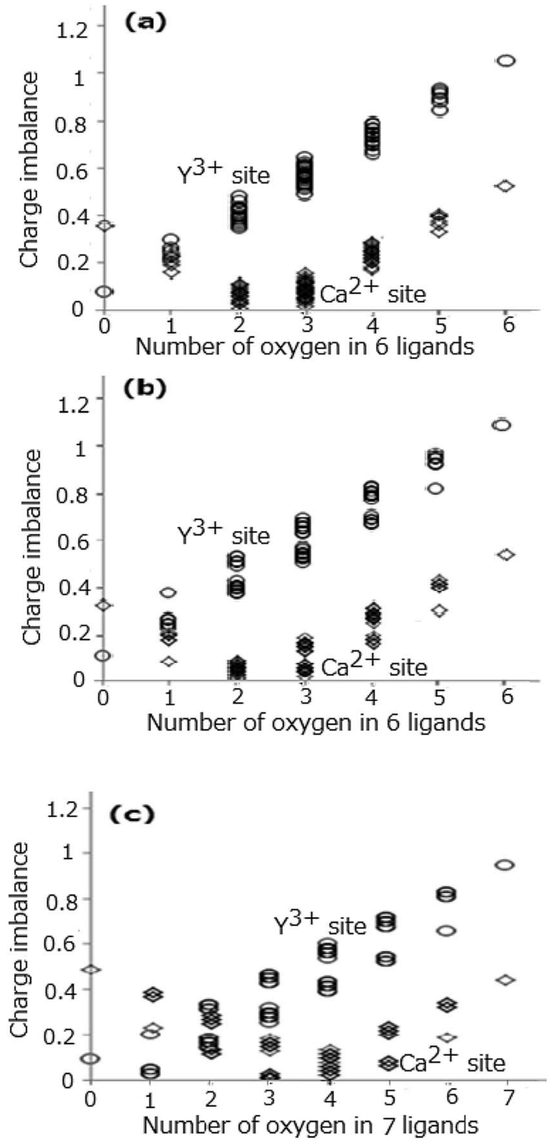

Fig. 4 Difference (charge imbalance) between the BVS and cation's valence at the Ln_1 site (a), Ln_2 site (b), and Ln_3 site (c), respectively.

value, is almost at the same level as total ratio O/(O + N) of CYSON, 21%, again. From the above consistent results, it is considered that one of the reason for successful extensive substitution of Y–N → Ca–O is an existence of the structure with the bond lengths much greater than the sum, 2.28 Å, of radii of Y^{3+} (CN:6) and O^{2-} ions yielding a smaller BVS, which leads to an increased oxygen coordination and the stabilization of charge distribution near the Ca^{2+} ions.

It is notable that the new type of calculation by use of Brown's BVS in this work shed light on the phenomenon, the substitution of O^{2-} for the N^{3-} site coordinating Ca^{2+} ions rather than Y^{3+} ions, because the phenomenon is consistent with the principle of ceramics that cations and anions are arranged so that local region forming electric charge as a sum might be minimized.

Table 6 The sets of O^{2-} and N^{3-} ligands providing the smallest three values of charge imbalance

Sets of $Y^{3+}/Ca^{2+}–O^{2-}/N^{3-}$	Values of charge imbalance
Y_1–[N_1, N_2, N_3, N_4, N_5, N_8]	0.0779
Y_1–[O_1, N_2, N_3, N_4, N_5, N_8]	0.2051
Y_1–[N_1, N_2, N_3, N_4, O_5, N_8]	0.2174
Ca_1–[N_1, O_2, O_3, N_4, N_5, N_8]	0.0042
Ca_1–[N_1, O_2, N_3, O_4, N_5, N_8]	0.0098
Ca_1–[O_1, N_2, N_3, N_4, O_5, O_8]	0.0174
Y_2–[N_1, N_2, N_3, N_4, N_5, N_9]	0.1131
Y_2–[O_1, N_2, N_3, N_4, N_5, N_9]	0.2322
Y_2–[N_1, O_2, N_3, N_4, N_5, N_9]	0.2466
Ca_2–[O_1, N_2, N_3, N_4, N_5, O_9]	0.0153
Ca_2–[O_1, O_2, N_3, N_4, O_5, N_9]	0.0262
Ca_2–[N_1, O_2, N_3, N_4, N_5, O_9]	0.0281
Y_3–[N_5, N_5, O_5, N_6, N_6, N_6, N_9]	0.0247
Y_3–[N_5, O_5, N_5, N_6, N_6, N_6, N_9]	0.0247
Y_3–[O_5, N_5, N_5, N_6, N_6, N_6, N_9]	0.0247
Ca_3–[N_5, N_5, O_5, N_6, N_6, O_6, O_9]	0.0076
Ca_3–[N_5, O_5, O_5, N_6, N_6, O_6, O_9]	0.0076
Ca_3–[O_5, N_5, O_5, N_6, N_6, O_6, O_9]	0.0076

Table 7 A set of anion ligands providing the minimum value of charge imbalance at each Si^{4+} site

A set of Si^{4+} and O/N ligands	Value of charge imbalance
Si_1–[O_7, N_1, N_4, N_6]	0.0331
Si_2–[O_2, N_1, N_4, N_5]	0.0914
Si_3–[O_5, N_1, N_3, N_6]	0.0036
Si_{4a}–[O_3, N_3, N_3, N_9]	0.0418
Si_{4b}–[O_3, N_3, N_3, N_7]	0.1536
Si_5–[O_2, N_2, N_2, N_8]	0.1287

4 Conclusions

The unique extensive substitution (about 70% of Y) of Y^{3+} → Ca^{2+} and N^{3-} → O^{2-} in the blue-excited yellow phosphor $(Y,Ca)_{6+x/3}Si_{11}(N,O)_{21}$:Ce was investigated by calculating the Brown's bond valence sums at each three Y/Ca/Ce cation sites, including all inequivalent positions. Due to the partial occupancy of the cation and anion sites in the "parent" CYSON structure, the coordination of anions at each cationic site was not known up to now. The obtained results for the first time allow to determine the number of anions of different kinds at each site. In particular, the number of the oxygen ligands is likely to be 0 at Y_1 and Y_2 sites and 2–3 at Ca_1 and Ca_2 sites, 0–1 at Y_3 site, and 3–4 at Ca_3 site. It indicates that the oxygen ions prefer to form coordination around the Ca ions rather than around the Y ions, which leads to a further conclusion that the Y–N bond should be extensively substituted by the Ca–O bond instead of agglomeration of the oxygen ions far apart from the Ca^{2+} ions. On the basis of the performed analysis, it became possible to find a chemically-based strong explanation for the successful extensive substitution of the Y–N pairs by the Ca–O pairs. It can be realized on account of formation of a stable structure having the bond lengths much greater than the simple sum (equal to 2.28 Å) of the ionic radii of the six-fold coordinated Y^{3+} and O^{2-} ions. Such substitution yields smaller BVS values and is accompanied by increased oxygen coordination and the stabilization of charge distribution near the Ca^{2+} ions. The performed analysis can be efficiently applied to other crystals with partial cation/anion occupancy or solid solutions; it helps to understand the local coordination around various sites in crystal lattice. The method acquires a special importance for the doped phosphor materials, since in this case the nearest coordination of an impurity ion determines the crystal field strength, point symmetry and, as such, the overall pattern of the crystal field splitting of impurity ions energy levels, and, finally, spectroscopic properties of such doped material.

Conflicts of interest

There are no conflicts to declare.

Acknowledgements

We are thankful to Samsung R&D Research Institute for the published details of CYSON. M.G. Brik thanks the supports from the Recruitment Program of High-end Foreign Experts (Grant No. GDW20145200225), the Programme for the Foreign Experts offered by Chongqing University of Posts and Telecommunications, Ministry of Education and Research of Estonia, Project PUT430, and European Regional Development Fund (TK141).

Notes and references

1 S. Nakamura and G. Fasol, *The blue laser diode: GaN Based Light Emitters and Lasers*, Springer, Berlin, 1997.

2 K. Uheda, N. Hirosaki, H. Yamamoto, H. Yamane, Y. Yamamoto, W. Inami and K. Tsuda, *The 206th Annual Meeting of the Electrochemical Society (Abstract No. 2073)*, Honolulu, Oct 3 2004.

3 N. Kijima, T. Seto and N. Hirosaki, *ECS Trans.*, 2009, **25**, 247–252.

4 H. A. Hoppe, H. Lutz, P. Morys, W. Schnick and A. Seilmeier, *J. Phys. Chem. Solids*, 2000, **61**, 2001–2006.

5 C. Hecht, F. Stadler, P. J. Schmidt, J. S. Gunne, V. Baumann and W. Schnick, *Chem. Mater.*, 2009, **21**, 1595–1601.

6 Y. Q. Li, A. C. A. Delising, G. de With and H. T. Hintzen, *Chem. Mater.*, 2005, **17**, 3242–3248.

7 R.-J. Xie, M. Mitomo, K. Uheda, F.-F. Xu and Y. Akimune, *J. Am. Ceram. Soc.*, 2002, **85**, 1229–1234.

8 N. Hirosaki, R.-J. Xie, K. Kimoto, T. Sekiguchi, Y. Yamamoto, T. Suehiro and M. Mitomo, *Appl. Phys. Lett.*, 2005, **86**, 211905.

9 Y. Liu, X. Zhang, Z. Hao, X. Wang and J. Zhang, *J. Mater. Chem.*, 2011, **21**, 6354–6358.

10 Y. Liu, J. Zhang, C. Zhang, J. Xu, G. Liu, J. Jiang and H. Jiang, *Adv. Opt. Mater.*, 2015, **3**, 1096–1101.

11 T. Seto and T. Izawa, *ECS J. Solid State Sci. Technol.*, 2015, **4**, R83–R88.

12 I. D. Brown, *Structure and Bonding in Crystals*, Academic Press, New York, 1981, vol. 2, pp. 1–30.

13 I. D. Brown and D. Altermatt, *Acta Crystallogr.*, 1985, **41**, 244–247.

14 N. E. Brese and M. O'Keeffe, *Acta Crystallogr.*, 1991, **47**, 192–197.

15 P. Dorenbos, *Phys. Rev. B: Condens. Matter Mater. Phys.*, 2000, **62**, 15640–15649.

16 P. E. D. Morgan, *J. Mater. Sci.*, 1986, **21**, 4305–4309.